frontiers in Physics

ORIGINAL RESEARCH
published: 11 August 2020
doi: 10.3389/fphy.2020.00237

Signal Improvement for Underwater Measurement of Metal Samples Using Collinear Long-Short Double-Pulse Laser Induced Breakdown Spectroscopy

Minchao Cui[1,2,3]*, *Yoshihiro Deguchi*[3,4]*, *Zhenzhen Wang*[3,4], *Changfeng Yao*[1], *Liang Tan*[1] *and Dinghua Zhang*[1]

[1] *MIIT Key Laboratory of High Performance Manufacturing for Aero Engine, Northwestern Polytechnical University, Xi'an, China,* [2] *Shaanxi Key Laboratory of Industrial Automation, Shaanxi University of Technology, Hanzhong, China,* [3] *Graduate School of Advanced Technology and Science, Tokushima University, Tokushima, Japan,* [4] *State Key Laboratory of Multiphase Flow in Power Engineering, Xi'an Jiaotong University, Xi'an, China*

OPEN ACCESS

Edited by:
Yufei Ma,
Harbin Institute of Technology, China

Reviewed by:
Vincenzo Palleschi,
Italian National Research Council, Italy
Fei Liu,
Zhejiang University, China

***Correspondence:**
Minchao Cui
cuiminchao@nwpu.edu.cn
Yoshihiro Deguchi
ydeguchi@tokushima-u.ac.jp

Specialty section:
This article was submitted to Optics and Photonics, a section of the journal Frontiers in Physics

Received: *18 March 2020*
Accepted: *29 May 2020*
Published: *11 August 2020*

Citation:
Cui M, Deguchi Y, Wang Z, Yao C, Tan L and Zhang D (2020) Signal Improvement for Underwater Measurement of Metal Samples Using Collinear Long-Short Double-Pulse Laser Induced Breakdown Spectroscopy. Front. Phys. 8:237. doi: 10.3389/fphy.2020.00237

We employed a collinear long-short double-pulse laser induced breakdown spectroscopy (LS-DP-LIBS) to detect the underwater metal samples. The emission spectra, time-resolved signal, plasma images and sound characteristics of plasma shockwaves are experimentally investigated in this work. The results show that the underwater signal of Al, Cu and Fe spectral lines are significantly improved by collinear LS-DP-LIBS with inter-pulse delay of 35 us. The mechanism of the signal improvement is considered to be the pre irradiation effect of the long pulse laser beam. In the collinear LS-DP-LIBS method, the long pulse first generates a cavitation bubble in water and provides a gaseous environment. Then the short pulse generates the plasma from the sample surface. The present experiments show that the collinear LS-DP-LIBS method offers a significant signal improvement in underwater measurement of metal samples. This new method has great potential in deep-sea exploration using LIBS.

Keywords: LIBS, long-short double-pulse, underwater, improvement, metals

INTRODUCTION

Laser-induced breakdown spectroscopy (LIBS) is a powerful tool for the exploring of the deep-sea [1]. In recent years, LIBS has attracted many researchers to work in the field of underwater measurement. A lot of studies have been concentrated on the development of the underwater LIBS measurement method. Yelameli et al. have investigated the classification of hydrothermal seafloor rocks using LIBS. Based on the proposed support vector machine method, the LIBS classification of rocks has obtained the accuracy of 98% [2]. Matsumoto et al. have proposed a non-gated detection method for underwater LIBS. By properly selecting the position, they have successfully obtained well-resolved spectral lines even without time-gated detection [3]. Wang et al. have proposed a low-pressure LIBS method for the sensitive detection of cesium in liquid [4]. Lan et al. have reported the detection improvement of solution measurement using a method to

measure the flame of alcohol-solution mixtures [5]. Jabbar et al. have proposed a calibration-free long-pulse duration LIBS method for the underwater measurement of metal alloys [6]. Li et al. have studied the salinity effects on the underwater LIBS [7]. Cui et al. have studied the Fraunhofer-type signal for underwater measurement of copper samples. Their results have suggested that the Fraunhofer-type signal can possibly be used for quantitative measurement of underwater LIBS [8]. Zhang et al. have proposed a capillary mode LIBS method to detect the elemental concentrations in solution. Their experimental results have shown that the accuracy of quantitative element analysis in liquids can be improved by the capillary mode LIBS [9]. Double-pulse LIBS (DP-LIBS) has been comprehensively studied by the research group of Giacomo. The basic mechanisms and model of DP-LIBS for underwater measurement have been revealed by theoretical analysis and experimental investigation [10, 11]. The effect of the cavitation bubble on plasma generation and evolution is considered to be a major reason for the improvement of underwater DP-LIBS [12]. The improved methods are still being widely studied for LIBS applications in the field of deep-sea exploration.

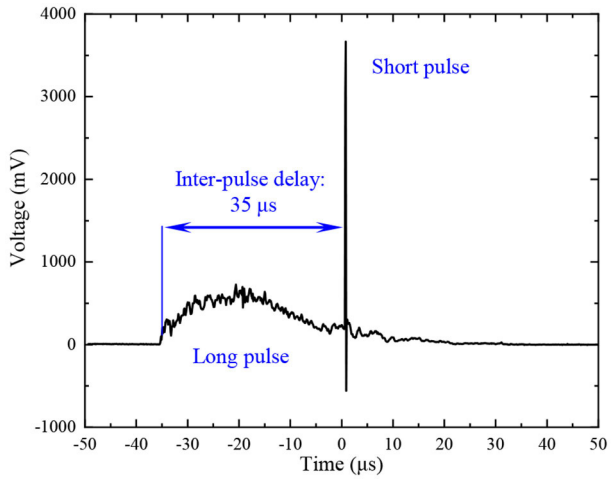

FIGURE 1 | Measured pulse shape of LS-DP-LIBS (LS-2145LIBS laser, inter-pulse delay: 35 μs).

In LIBS data processing, the intensity of the emission line is used to analyze the elemental concentration. Generally, the emission lines can be observed in the LIBS spectrum with a gate delay time of several microseconds [13, 14]. Based on time-resolved studies on the emission spectra, the optimized delay time can be selected to record a LIBS signal well [15]. In fact, it is easy to record the LIBS signal well in air or a vacuum atmosphere because the laser-induced plasma has a relatively long lifetime in these cases [16]. However, it is quite difficult to record a satisfactory spectrum in underwater LIBS measurement. Underwater laser-induced plasma suffers from several drawbacks due to the cooling and pressure effect of water. Yoshino et al. have reported the weak intensity of deep-sea laser-induced plasma. They have proposed a signal pre-processing method based on artificial neural networks to improve the LIBS measurement results [17]. Michel et al. [18] and Thornton and Ura [19] have studied the rapid decay and large fluctuation problems of underwater LIBS. They held the view that the effect of water pressure should be a concern in underwater LIBS. The lifetime of laser-induced plasma is usually several microseconds in an air atmosphere, but it is only hundreds of nanoseconds in a

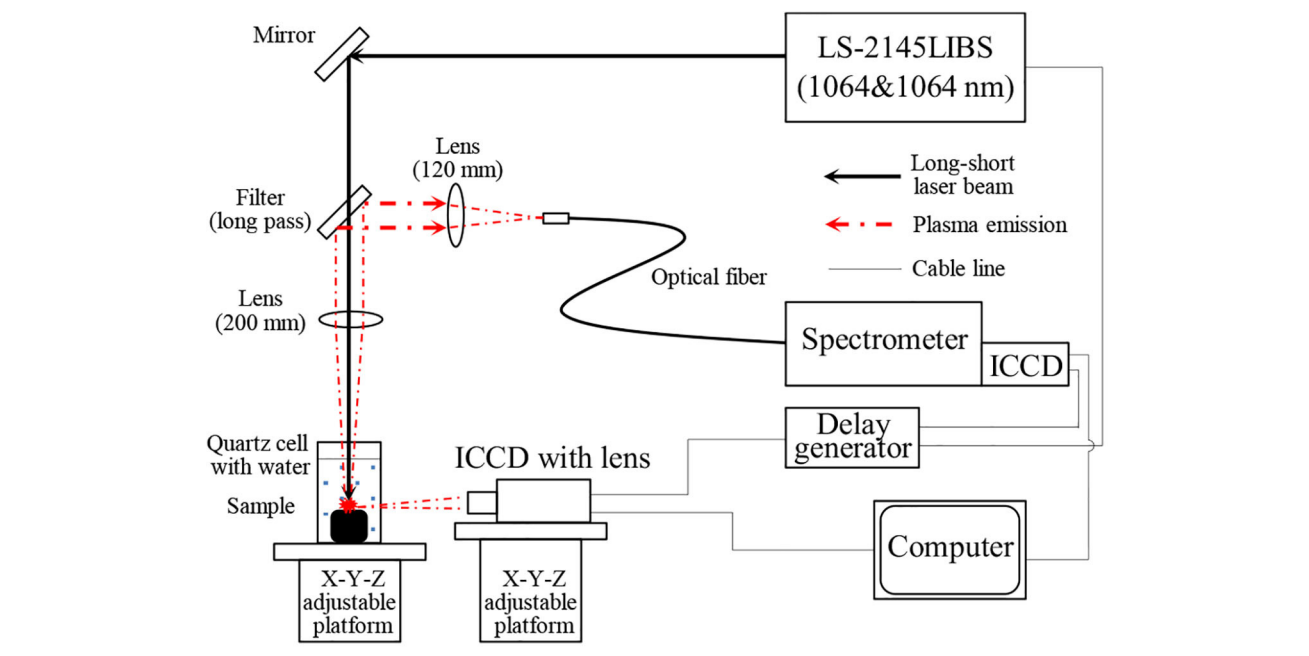

FIGURE 2 | Experimental setup of LIBS system for underwater measurement.

water environment [20]. The emission of laser-induced plasma is affected by the negative influences of water [21]. Therefore, signal improvement is one of the vital issues for underwater LIBS. In previous literature of underwater LIBS, De Giacomo et al. [22, 23] and Gavrilovic et al. [24, 25] have reported a signal improvement using a double-pulse (two nanosecond pulses), meanwhile, Jabbar et al. [6], Sakka et al. [26] and Oguchi et al. [27] have reported a signal improvement using a single-pulse with long-pulse-duration. The experimental results of these studies had shown that the reason for signal improvement is related to the cavitation bubble in an underwater environment. Both the double-pulse and long-duration-pulse can produce a beneficial effect for underwater LIBS. Inspired by these studies, the experimental results of underwater measurement are investigated in this work using a long and short double-pulse LIBS method.

The long and short double-pulse LIBS method was proposed by our group and it has been named as LS-DP-LIBS [28, 29]. In previous studies [30, 31], LS-DP-LIBS has been compared with SP-LIBS based on the measurement results in an air atmosphere. Those studies have demonstrated that the plasma is enhanced and stabilized by LS-DP-LIBS. The enhancement and stabilization are owing to the heating effect of long pulse during the plasma generation and evolution stages. In this work, the +collinear LS-DP-LIBS method is used to measure the underwater metal samples. The spectra characteristics, time-resolved signal, plasma images and plasma shockwave are experimentally investigated. The mechanism of signal improvement in underwater measurement is discussed through the comparative study between SP-LIBS and LS-DP-LIBS.

EXPERIMENTAL SETUP

The long-short double-pulse laser beams are generated by a special laser (LOTIS TII, LS-2145LIBS), which is co-developed by our group and Tokyo Instrument Co. Ltd. The laser head consists of two independent channels: Channel 1 without Q-switched unit and Channel 2 with Q-switched unit. The output beams of these two channels are combined inside the laser head and output from the same external telescope. The detailed optical diagram of LS-2145LIBS laser is available in the experimental section of our previous paper [8]. In addition, in order to measure the pulse shape of the LS-2145LIBS laser, a Si photodiode

TABLE 1 | Elemental composition of Al sample (mass fraction, %).

Al	Fe	Si	Cu	Zn	Ti
99.95	0.004	0.002	0.002	0.004	0.002

TABLE 2 | Elemental composition of Cu sample (mass fraction, %).

Cu	Sb	P	S	Zn	As	Ni	Fe	Pb
99.95	0.002	0.002	0.004	0.002	0.002	0.002	0.004	0.004

TABLE 3 | Elemental composition of Fe sample (mass fraction, %).

Fe	C	S	P	Si	Mn	Cr	Ni
99.74	0.003	0.005	0.004	0.003	0.032	0.005	0.016

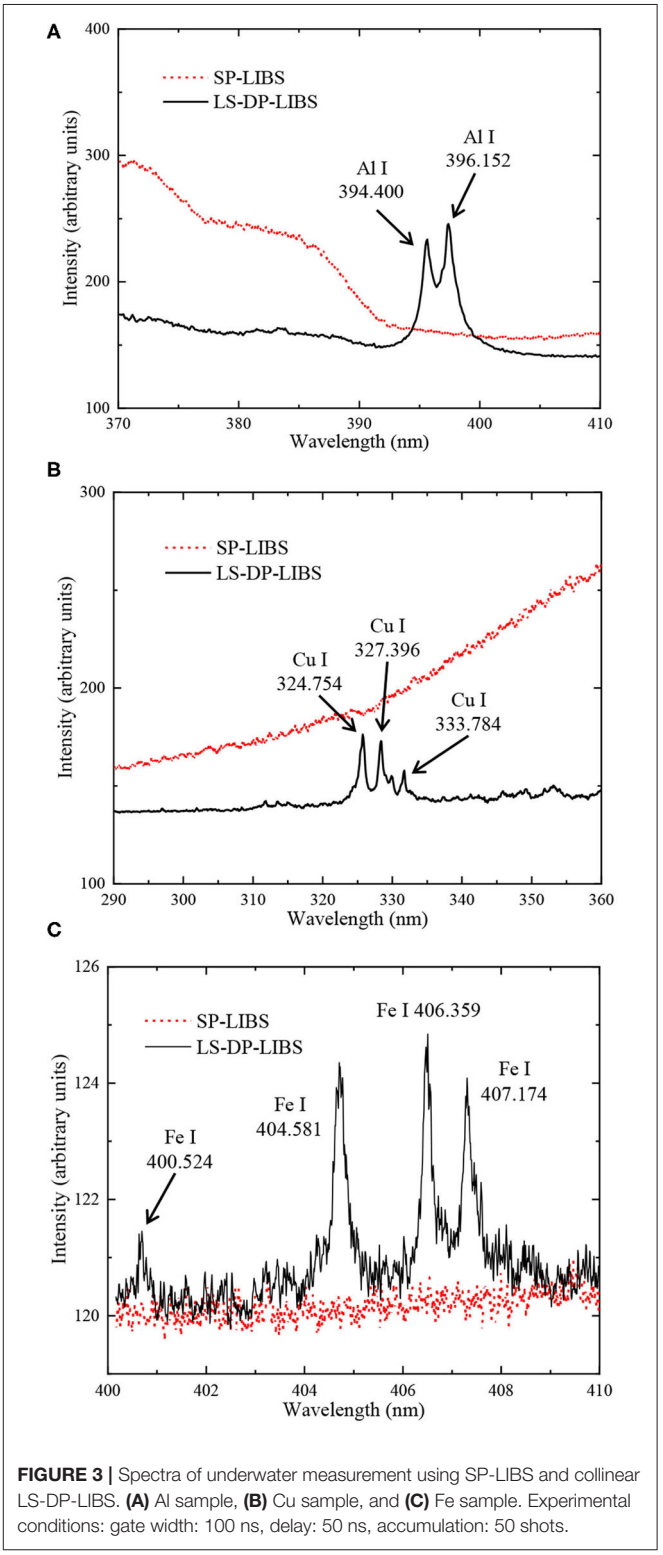

FIGURE 3 | Spectra of underwater measurement using SP-LIBS and collinear LS-DP-LIBS. **(A)** Al sample, **(B)** Cu sample, and **(C)** Fe sample. Experimental conditions: gate width: 100 ns, delay: 50 ns, accumulation: 50 shots.

sensor (Hamamatsu, S1336-18BQ) was placed near the light path. The scattered laser light was converted to electric signal by the sensor. Meanwhile, an oscilloscope (Tektronix, MDO3014) was employed to record the output voltage of the sensor. **Figure 1** shows the measured pulse shape of LS-2145LIBS laser. The pulse energy of short pulse was set to 25 mJ with the pulse duration of 6–7 ns (FWHM) and the pulse energy of long pulse was set to 100 mJ with the total pulse duration of 35 μs. Meanwhile, the inter-pulse delay between the trigger timings of long pulse and short pulse was configured to 35 μs in this work. In this study, the irradiance of short pulse was around 2.0 Gw/cm^2 and the irradiance of long pulse was around 2.5 × 10^{-3} GW/cm^2. From this point, the long pulse laser beam can also be transmitted through optical fiber in the practical undersea application.

Figure 2 illustrates the LIBS system which was employed to carry out the underwater experiments in the present work. The long-short double-pulse laser beam was reflected by a mirror and focused to the sample by a lens (focal length: 200 mm). The plasma light was collected to the fiber entrance in the reverse direction. Next, the emission light of plasma was dispersed by a spectrometer (SOL, NP-250-2M, CH1: 600 lines/mm, CH2: 3,600 lines/mm) and detected by an ICCD (Andor, iStar DH334T-18U-03). To observe the plasma plume simultaneously, another ICCD (Andor, iStar DH334T-18U-03) with a camera lens (Nikon, 602095, focal length: 35 mm) was placed on an X-Y-Z adjustable platform to record the plasma images. The trigger timings of the two laser channels and two ICCD are controlled by a delay generator (Stanford Research Systems, DG645). The quartz cell with the deionized water and metal sample was fixed on an X-Y-Z adjustable platform and automatically driven by motors with a scanning motion in the X-Y plane. During the LIBS measurement, the distance from the water surface to the sample surface was around 100 mm.

The metal samples with high-purity aluminum (Al), copper (Cu) and iron (Fe) composition were used as measuring targets in the present study. All of the 3 samples were used to carry out the underwater LIBS acquiring, and the results are discussed in section Spectral Characteristics and Time-Resolved Intensity. The Cu sample was used to conduct the recording of plasma images, 1-shot spectra and sound signal. The corresponding results are discussed in section Plasma Images and Characteristics of Plasma Shockwave. The reference compositions of the samples, which were provided

TABLE 4 | Parameters of the specific atomic emission lines [32].

Line name	E_i (cm^{-1})*	E_k (cm^{-1})*
Cu I 324.754 nm	0	30,783.697
Cu I 327.396 nm	0	30,535.324
Cu I 333.784 nm	11,202.618	41,153.470
Al I 394.400 nm	0	25,347.756
Al I 396.152 nm	112.061	25,347.756
Fe I 400.524 nm	12,560.934	37,521.161
Fe I 404.581 nm	11,976.239	36,686.176
Fe I 406.359 nm	12,560.934	37,162.746
Fe I 407.174 nm	12,968.554	37,521.161

E_i, lower energy level; E_k, upper energy level.

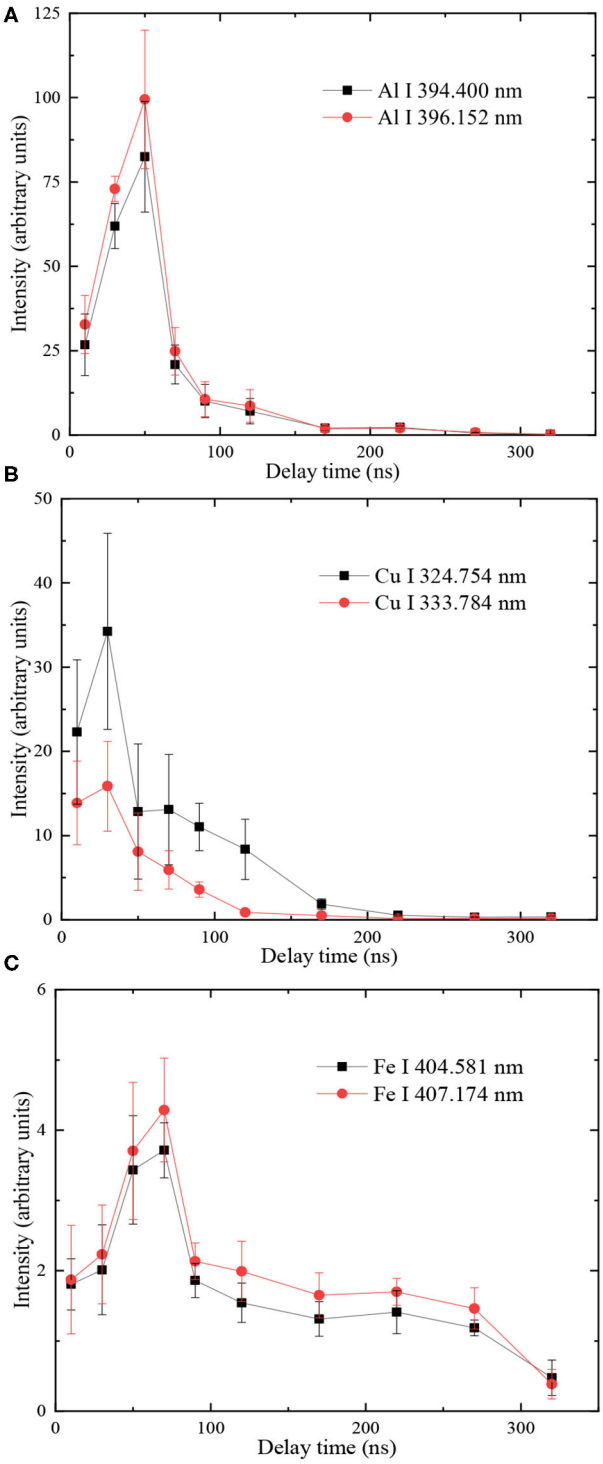

FIGURE 4 | Time-resolved intensity of collinear LS-DP-LIBS. **(A)** Al sample, **(B)** Cu sample, and **(C)** Fe sample. Experimental conditions: gate width: 100 ns, accumulation: 50 shots, repetition of experiments: 5 times.

by Kojundo Chemical Laboratory Co., Ltd., Japan, are listed in **Tables 1–3**, respectively.

RESULTS AND DISCUSSION

Spectral Characteristics

In this study, the comparative experiments were carried out using SP-LIBS and collinear LS-DP-LIBS. **Figures 3A–C** present the measured results from the underwater Al sample, the Cu sample and the Fe sample, respectively. **Table 4** provides the parameters of the spectral lines which can be distinguished in **Figure 3** [32]. The signal of SP-LIBS is characterized by the noise with continuous background. This type of background is often observed in underwater LIBS studies [3, 7, 17, 18, 26]. The formation of continuous background can be attributed to the ablation of water molecules during the LIBS process. In the underwater environment, the nanosecond pulsed laser beam is able to ablate the material on sample surface as well as the water molecules in its surroundings. The ablation of water molecules leads to the significant continuous background in the spectrum. Generally, the emission spectral lines corresponding to the sample elements can still be distinguished from the continuous background in most of the underwater LIBS studies with relatively high laser pulse energy [21, 26, 27]. However, the spectral lines were completely submerged in the background and noise in the present results of SP-LIBS. The reason is considered to be the low energy of the short pulse laser beam used in this work. Considering the practical application in deep-sea exploration, the energy of the short pulse was set to 25 mJ per pulse in this study. In this case, the laser head can be designed in a compact size and sent to undersea environments for LIBS measurement. The low pulse energy had significantly reduced the signal quality of underwater LIBS measurement. As for the LS-DP-LIBS method, the peak power of the additional long pulse was very low compared to the nanosecond laser pulse. Therefore, the generation and transmission of a long pulse laser beam was easier than short pulse laser beam. The instrument strategy of undersea LS-DP-LIBS can use either of the following two methods: One way is to integrate an independent laser channel in the nanosecond laser head, which is same to the LS-2145LIBS laser in this work; another way is to transmit the long pulse beam, which can be generated by another laser on the mother ship, to the undersea optical system through optical fiber.

According to **Figure 3**, the spectra of collinear LS-DP-LIBS are obviously different from the spectra of SP-LIBS. The specific spectral lines of Al, Cu, and Fe elements can be distinguished in the spectra of LS-DP-LIBS. The continuous background is significantly reduced. The characteristics of the spectra are similar to the measurement results in the air atmosphere. The spectral characteristics suggest that the mechanisms of SP-LIBS and LS-DP-LIBS are different in the

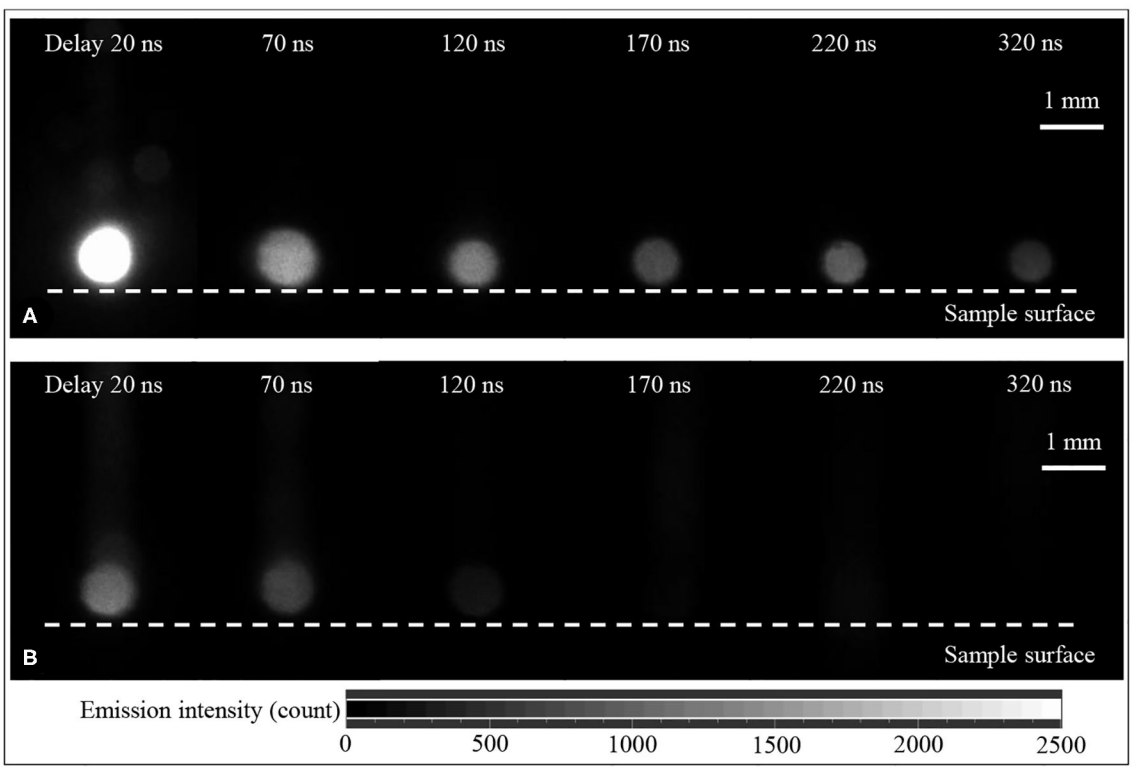

FIGURE 5 | Plasma images of underwater LIBS measurement. **(A)** Collinear LS-DP-LIBS and **(B)** conventional SP-LIBS. Experimental conditions: gate width: 100 ns, accumulation: 1 shot.

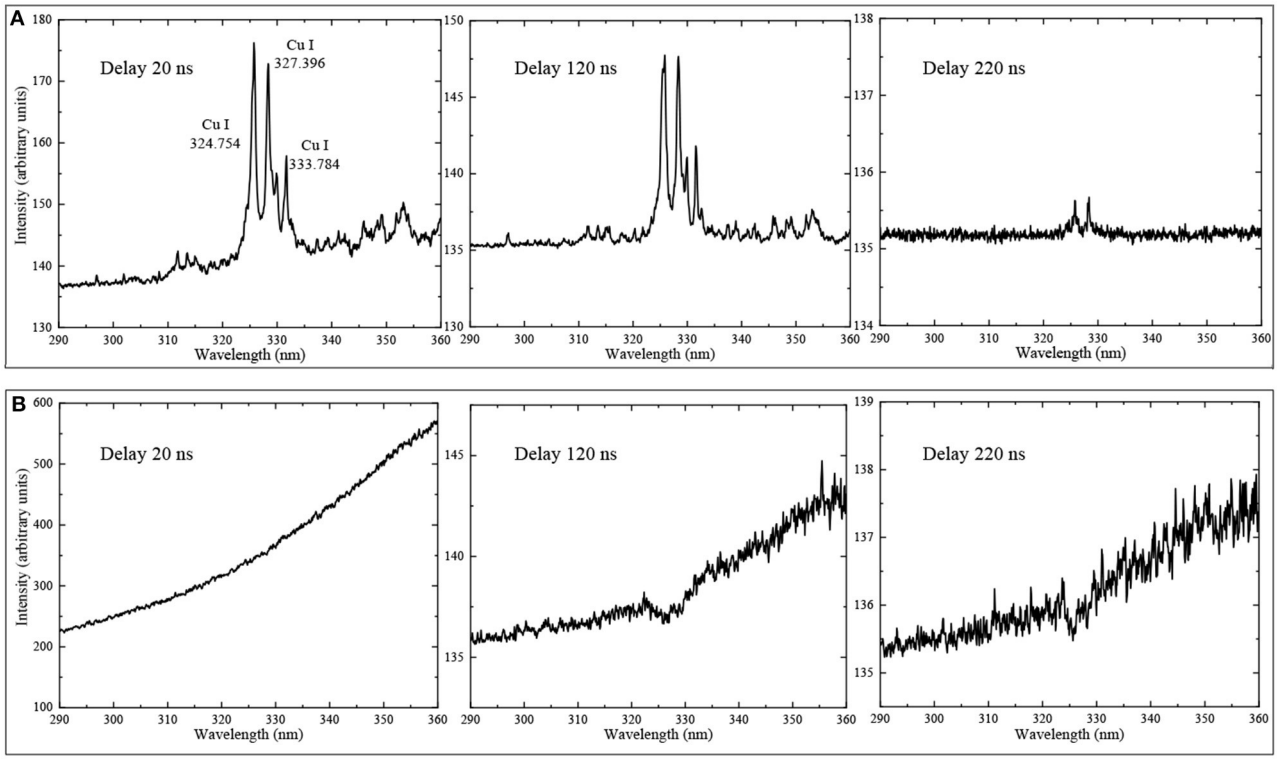

FIGURE 6 | 1-Shot spectra of underwater Cu sample in different delays. **(A)** Collinear LS-DP-LIBS and **(B)** conventional SP-LIBS. Experimental conditions: gate width: 100 ns, accumulation: 1 shot.

case of underwater measurement. The recorded spectra have demonstrated that the signal quality is improved by the collinear LS-DP-LIBS.

Time-Resolved Intensity

Figure 4 shows the time-resolved intensity of collinear LS-DP-LIBS. **Figures 4A–C** presents the results which were measured from Al, Cu and Fe samples, respectively. It can be seen that the time-resolved intensities show the consistent trend for different spectral lines and different samples. As the delay increases from 10 ns, the intensity of the spectral line increases to the maximum value in tens of nanoseconds. After that, the intensity continuously decreases over a relatively wide delay range. This phenomenon is very similar to the phenomenon of LIBS measurement in the air. The results also show that the delay value corresponding to the maximum intensity is different for different samples. It is related to the absorption process of laser energy and the ablation threshold of the sample materials [25].

Plasma Images

The plasma morphology was also investigated in this study. The plasma images in different delays were recorded by the ICCD, as shown in **Figure 5**. The upper images show the plasma characteristics of collinear LS-DP-LIBS. The plasma generated by LS-DP-LIBS has a spherical structure, as shown in **Figure 5A**. The emission intensity and spatial size of plasma decrease as the delay increases. **Figure 5B** shows the plasma images of conventional SP-LIBS. It can be seen that the emission intensity of the plasma is significantly weaker than LS-DP-LIBS. The plasma emission is unobservable when the delay is longer than 170 ns in SP-LIBS condition, but it is still observable when the delay is 320 ns in LS-DP-LIBS condition. This result indicates that the signal improvement of LS-DP-LIBS can be attributed to the emission enhancement and the lifetime extension of plasma.

Figure 6 provides the recorded spectral results which correspond to the plasma images in **Figure 5**. The spectra were acquired with the 1-shot accumulation. As shown in **Figure 6A**, the spectral lines at Cu I 324.754, Cu I 327.396, and Cu I 333.784 nm can be clearly distinguished from the continuous background and noise in the LS-DP-LIBS condition. **Figure 6B** shows the results in the SP-LIBS condition. It can be seen that the spectra are obviously different. The signal is dominated by continuous background and noise. No clear spectral line can be distinguished in the spectra of SP-LIBS.

According to the images in **Figure 5**, the emission intensity of plasma is almost at the same level in the following two experimental conditions: delay 120 ns of LS-DP-LIBS and delay 20 ns of SP-LIBS. According to the spectra of LS-DP-LIBS (**Figure 6A**), the spectral lines of the Cu element acquired the strong signal quality in the delay of 120 ns. However, the spectral lines are unable to be clearly separated in the SP-LIBS spectrum with a delay parameter of 20 ns due to the strong

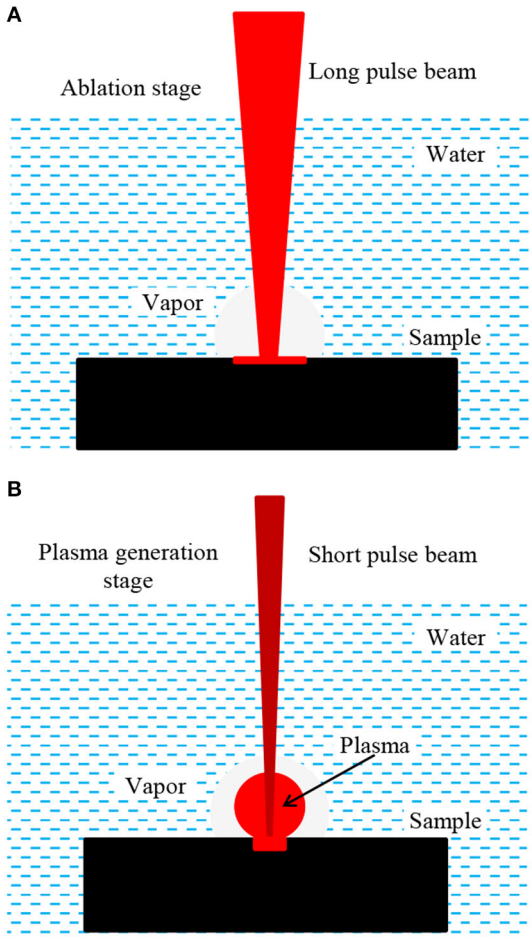

FIGURE 7 | Principle model of underwater measurement using collinear LS-DP-LIBS. **(A)** Ablation stage of long pulse and **(B)** plasma generation stage of short pulse.

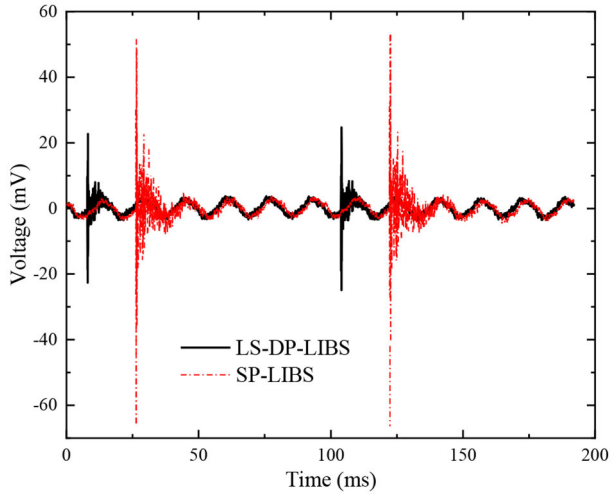

FIGURE 8 | Output voltage of sound sensor during the underwater LIBS experiments.

continuous background and noise, as shown in **Figure 6B**. This result suggests that the mechanism of signal improvement is also related to the reduction of background emission in the LS-DP-LIBS condition.

Characteristics of Plasma Shockwave

Figure 7 shows the principle model of underwater LS-DP-LIBS measurement, which is proposed based on the literature of underwater double-pulse LIBS [11, 33]. Basically, the whole process can be divided into two stages: the ablation stage of long pulse (**Figure 7A**) and the plasma generation stage of short pulse (**Figure 7B**). In collinear LS-DP-LIBS, the long pulse beam is firstly irradiated on the sample surface. Generally, the peak power of long pulse is below the ablation threshold of sample material. Therefore, the long pulse is unable to generate observable plasma. Nevertheless, the long pulse can produce a significant heating effect on the focus area because it irradiates 100 mJ per pulse to the focus spot in 35 μs (irradiance: around 2.5×10^{-3} GW/cm^2). The laser energy is absorbed by the surrounding water then a cavitation bubble is formed on the sample surface, as shown in **Figure 7A**. Next, the short pulse beam is irradiated to the sample and the plasma is generated inside the gaseous environment instead of the underwater environment. The generation and evolution processes of plasma are carried out inside the cavitation bubble, as shown in **Figure 7B**. Therefore, the negative influences of underwater measurement can be reduced and the plasma state is close to that of air measurement. The role of the cavitation bubble has also been noted in the short and short double pulse LIBS studies [10–12, 22–25, 34]. In this study, a similar effect is obtained by the long pulse laser beam which is output through operating the laser channel at free running mode. The generation of long pulse does not require a Q-switched unit, which can reduce the instrument complexity and cost.

In order to find the evidence to support the above model, a sound sensor (YAV Z2, Wuhan Yawei Co., Ltd., China) was placed on the quartz cell to record the acoustic signal generated by the plasma shockwave. **Figure 8** shows the output voltage of the sound sensor during collinear LS-DP-LIBS and SP-LIBS experiments. The background signals are sinusoidal waveform with high frequency in both conditions. However, the maximum peak-to-peak value of SP-LIBS is significantly larger than that of LS-DP-LIBS. Meanwhile, the voltage magnitude of SP-LIBS is also significantly larger than that of LS-DP-LIBS. This phenomenon is consistent with the principle model in **Figure 7**. In the case of LS-DP-LIBS, the plasma is generated inside the cavitation bubble which is created by long pulse laser beam. Thus, the plasma shockwave is significantly attenuated while passing through the gaseous gap and the gas-liquid interface. This mechanism causes the detected sound intensity to be smaller in the LS-DP-LIBS condition. The present experimental result provides effective evidence to show that the long pulse creates a gaseous environment for plasma generation in LS-DP-LIBS.

CONCLUSIONS

1. For Al, Cu, and Fe samples, the spectra of underwater SP-LIBS show the characteristics of continuous background and noise in a delay of 50 ns. However, the spectra with clear spectral lines can be acquired by the underwater LS-DP-LIBS in the same delay. The continuous background of underwater LIBS measurement is significantly reduced by the collinear LS-DP-LIBS method. According to the time-resolved intensity of spectral lines, the phenomenon of underwater LS-DP-LIBS is very similar to the phenomenon of LIBS measurement in the air. The experimental results suggest that the long pulse beam provides a gaseous environment for plasma generation and evolution in the underwater LS-DP-LIBS measurement process.
2. According to the investigation of plasma morphology, the underwater plasma generated by collinear LS-DP-LIBS is a spherical structure with strong emissions. The time-resolved plasma images indicate that the signal improvement of LS-DP-LIBS can be attributed to the emission enhancement and the lifetime extension of plasma. Meanwhile, the time-resolved 1-shot spectra suggest that the mechanism of signal improvement by LS-DP-LIBS is also related to the reduction of background emission of plasma.
3. The signal improvement of LS-DP-LIBS is attributed to the effects of the cavitation bubble in underwater measurement. In the collinear LS-DP-LIBS process, the long pulse beam firstly generates the cavitation bubble in water and provides a gaseous environment. Then, the short pulse beam generates plasma inside the bubble. This mechanism is supported by the sound detection results of plasma shockwaves. The detected sound intensity of LS-DP-LIBS is significantly smaller than that of SP-LIBS, which is caused by the attenuation effect of gaseous gap and gas-liquid interface.

DATA AVAILABILITY STATEMENT

The raw data supporting the conclusions of this article will be made available by the authors, without undue reservation.

AUTHOR CONTRIBUTIONS

MC: investigation, writing—original draft preparation, and data curation. YD: supervision, conceptualization, and methodology. ZW: methodology and validation. CY: methodology, writing—reviewing, and editing. LT: investigation, writing—reviewing, and editing. DZ: writing—reviewing, editing, and supervision. All authors contributed to the article and approved the submitted version.

FUNDING

This work was supported by National Natural Science Foundation of China for Key Program (Grant No. 91860206), National Natural Science Foundation of China (Grant No. 51875472), National Science and Technology Major Project (Grant No. 2017-VII-0001-0094), China Postdoctoral Science Foundation (Grant No. 2019M663823), and Opening Foundation of Shaanxi University of Technology Shaanxi Key Laboratory of Industrial Automation (Grant No. SLGPT2019KF01-19).

REFERENCES

1. Laserna J, Vadillo JPM, Purohit P. Laser-Induced Breakdown Spectroscopy (LIBS): fast, effective, and agile leading edge analytical technology. *Appl Spectrosc*. (2018) **72**:35–50. doi: 10.1177/0003702818791926
2. Yelameli M, Thornton B, Takahashi T, Weerakoon T, Ishii K. Classification and statistical analysis of hydrothermal seafloor rocks measured underwater using laser-induced breakdown spectroscopy. *J Chemometr*. (2019) **33**:e3092. doi: 10.1002/cem.3092
3. Matsumoto A, Tamura A, Fukami K, Ogata YH, Sakka T. Single-pulse underwater laser-induced breakdown spectroscopy with nongated detection scheme. *Anal Chem*. (2013) **85**:3807–11. doi: 10.1021/ac400319v
4. Wang ZZ, Yan JJ, Liu JP, Deguchi Y, Katsumori S, Ikutomo A. Sensitive cesium measurement in liquid sample using low-pressure laser-induced breakdown spectroscopy. *Spectrochim Acta Part B*. (2015) **114**:74–80. doi: 10.1016/j.sab.2015.10.006
5. Lan YJ, Lu Y, Dong XY, Zheng R. Detection improvement of laser-induced breakdown spectroscopy using the flame generated from alcohol-solution mixtures. *Opt Express*. (2007) **27**:29896–904. doi: 10.1364/OE.27.029896
6. Jabbar A, Hou Z, Liu JC, Ahmed R, Mahmood S, Wang Z. Calibration-free analysis of immersed metal alloys using long-pulse-duration laser-induced breakdown spectroscopy. *Spectrochim Acta Part B*. (2019) **157**:84–90. doi: 10.1016/j.sab.2019.05.013
7. Li N, Guo JJ, Zhang C, Zhang YQ, Li QY, Tian Y, et al. Salinity effects on elemental analysis in bulk water by laser-induced breakdown spectroscopy. *Appl Opt*. (2019) **58**:3886–91. doi: 10.1364/AO.58.003886
8. Cui M, Deguchi Y, Wang Z, Tanaka S, Xue B, Yao C, et al. Fraunhofer-type signal for underwater measurement of copper sample using collinear long-short double-pulse laser-induced breakdown spectroscopy. *Spectrochim Acta Part B*. (2020) **168**:105873. doi: 10.1016/j.sab.2020.105873
9. Zhang DC, Hu ZQ, Su YB, Hai B, Zhu XL, Zhu JF, et al. Simple method for liquid analysis by laser-induced breakdown spectroscopy (LIBS). *Opt Express*. (2018) **6**:18794–802. doi: 10.1364/OE.26.018794
10. De Giacomo A, Dell'Aglio M, Colao F, Fantoni R. Double pulse laser produced plasma on metallic target in seawater: basic aspects and analytical approach. *Spectrochim Acta Part B*. (2004) **59**:1431–8. doi: 10.1016/j.sab.2004.07.002
11. Casavola A, De Giacomo A, Dell'Aglio M, Taccogna F, Colonna G, Pascale OD, et al. Experimental investigation and modelling of double pulse laser induced plasma spectroscopy under water. *Spectrochim Acta Part B*. (2005) **60**:975–85. doi: 10.1016/j.sab.2005.05.034
12. López-Claros M, Dell'Aglio M, Gaudiuso R, Santagata A, De Giacomo A, Fortes FJ, et al. Double pulse laser induced breakdown spectroscopy of a solid in water: Effect of hydrostatic pressure on laser induced plasma, cavitation bubble and emission spectra. *Spectrochim Acta Part B*. (2017) **133**:63–71. doi: 10.1016/j.sab.2017.02.010
13. Miziolek A, Palleschi V, Schechter I. *Laser-Induced Breakdown Spectroscopy (LIBS)*. New York, NY: Cambridge University Press. (2006).
14. Cui MC, Deguchi Y, Wang ZZ, Tanaka S, Jeon MG, Fujita Y, et al. Remote open-path laser-induced breakdown spectroscopy for the analysis of manganese in steel samples at high temperature. *Plasma Sci Technol*. (2019) **21**:034007. doi: 10.1088/2058-6272/aaeba7
15. Zaytsev SM, Popov AM, Labutin TA. Stationary model of laser-induced plasma: critical evaluation and applications. *Spectrochim Acta Part B*. (2019) **158**:105632. doi: 10.1016/j.sab.2019.06.002

16. Ma Y, He Y, Sampaolo A, Qiao S, Yu X, Tittel FK, et al. Ultra-high sensitive trace gas detection based on light-induced thermoelastic spectroscopy and a custom quartz tuning fork. *Appl Phys Lett*. (2020) **116**:011103. doi: 10.1063/1.5129014
17. Yoshino S, Thornton B, Takahashi T, Takaya Y, Nozaki T. Signal preprocessing of deep-sea laser-induced plasma spectra for identification of pelletized hydrothermal deposits using artificial neural networks. *Spectrochim Acta Part B*. (2018) **145**:1–7. doi: 10.1016/j.sab.2018.03.015
18. Michel AP, Lawrence-Snyder M, Angel SM, Chave AD. Laser-induced breakdown spectroscopy of bulk aqueous solutions at oceanic pressures: evaluation of key measurement parameters. *Appl Opt*. (2007) **46**:2507–15. doi: 10.1364/AO.46.002507
19. Thornton B, Ura T. Effects of pressure on the optical emissions observed from solids immersed in water using a single pulse laser. *Appl Phys Express*. (2011) **4**:022702. doi: 10.1143/APEX.4.022702
20. Ma Y, Qiao S, Patimisco P, Sampaolo A, Wang Y, Tittel FK, et al. In plane quartz-enhanced photoacoustic spectroscopy. *Appl Phys Lett*. (2020) **116**:061101. doi: 10.1063/1.5142330
21. Tian Y, Hou SY, Wang LT, Duan XJ, Xue BY, Lu Y, et al. CaOH molecular emissions in underwater laser-induced breakdown spectroscopy: spatial–temporal characteristics and analytical performances. *Anal Chem*. (2019) **21**:13970–7. doi: 10.1021/acs.analchem.9b03513
22. De Giacomo A, Dell'Aglio M, Colao F, Fantoni R, Lazic V. Double-pulse LIBS in bulk water and on submerged bronze samples. *Appl Surf Sci*. (2005) **247**:157–62. doi: 10.1016/j.apsusc.2005.01.034
23. De Giacomo A, Dell'Aglio M, Casavola A, Colonna G, De Pascale O, Capitelli M. Elemental chemical analysis of submerged targets by double-pulse laser-induced breakdown spectroscopy. *Anal Bioanal Chem*. (2006) **385**:303–11. doi: 10.1007/s00216-006-0323-7
24. Gavrilovic MR, Cvejic M, Lazic V, Jovicevic S. Secondary plasma formation after single pulse laser ablation underwater and its advantages for laser induced breakdown spectroscopy (LIBS). *Phys Chem Chem Phys*. (2016) **18**:14629–37. doi: 10.1039/C6CP01515H
25. Gavrilovic MR, Lazic V, Jovicevic S. Influence of the target material on secondary plasma formation underwater and its laser induced breakdown spectroscopy (LIBS) signal. *J Anal At Spectrom*. (2017) **32**:345–53. doi: 10.1039/C6JA00300A
26. Sakka T, Tamura A, Matsumoto A, Fukami K, Nishi N, Thornton B. Effects of pulse width on nascent laser-induced bubbles for underwater laser-induced breakdown spectroscopy. *Spectrochim Acta Part B*. (2014) **97**:94–8. doi: 10.1016/j.sab.2014.05.009
27. Oguchi H, Sakka T, Ogata YH. Effects of pulse duration upon the plume formation by the laser ablation of Cu in water. *J Appl Phys*. (2007) **102**:023306. doi: 10.1063/1.2759182
28. Wang Z, Deguchi Y, Liu R, Ikutomo A, Zhang Z, Chong D, et al. Emission characteristics from laser-induced plasma using collinear long and short dual-pulse LIBS. *Appl Spectrosc*. (2017) **71**:2187–98. doi: 10.1177/0003702817693239
29. Cui M, Deguchi Y, Wang Z, Fujita Y, Liu R, Shiou FJ, et al. Enhancement and stabilization of plasma using collinear long-short double-pulse laser-induced breakdown spectroscopy. *Spectrochim Acta Part B*. (2018) **142**:14–22. doi: 10.1016/j.sab.2018.02.002
30. Cui M, Deguchi Y, Wang Z, Tanaka S, Fujita Y, Zhao S. Improved analysis of manganese in steel samples using collinear long–short double pulse Laser-Induced Breakdown Spectroscopy (LIBS). *Appl Spectrosc*. (2019) **73**:152–62. doi: 10.1177/0003702818803943
31. Cui M, Deguchi Y, Yao C, Wang Z, Tanaka S, Zhang D. Carbon detection in solid and liquid steel samples using ultraviolet long-short double pulse laser-induced breakdown spectroscopy. *Spectrochim Acta Part B*. (2020) **167**:105839. doi: 10.1016/j.sab.2020.105839
32. *National Institute of Standards and Technology, NIST Standard Reference Database 78*. (2019). Available online at: http://physics.nist.gov/PhysRefData/ASD/lines_form.html (accessed December 30, 2019).
33. De Giacomo A, Dell'Aglio M, Pascale OD, Capitelli M. From single pulse to double pulse ns-laser induced breakdown spectroscopy under water: elemental analysis of aqueous solutions and submerged solid samples. *Spectrochim Acta Part B*. (2007) **62**:721–38. doi: 10.1016/j.sab.2007.06.008
34. Walsh N, Costello JT, Kelly TJ. Optical diagnostics of laser-produced aluminium plasmas under water. *Appl Phys B*. (2017) **123**:179. doi: 10.1007/s00340-017-6754-3

Conflict of Interest: The authors declare that the research was conducted in the absence of any commercial or financial relationships that could be construed as a potential conflict of interest.

Copyright © 2020 Cui, Deguchi, Wang, Yao, Tan and Zhang. This is an open-access article distributed under the terms of the Creative Commons Attribution License (CC BY). The use, distribution or reproduction in other forums is permitted, provided the original author(s) and the copyright owner(s) are credited and that the original publication in this journal is cited, in accordance with accepted academic practice. No use, distribution or reproduction is permitted which does not comply with these terms.